ELSEVIER

Low-energy vibrational modes in phenylene oligomers studied by THz time-domain spectroscopy

M.B. Johnston [a],*, L.M. Herz [b], A.L.T. Khan [b], A. Köhler [b], A.G. Davies [c], E.H. Linfield [b]

[a] *Clarendon Laboratory, University of Oxford, Parks Road, Oxford OX1 3PU, UK*
[b] *Cavendish Laboratory, University of Cambridge, Madingley Road, Cambridge CB3 0HE, UK*
[c] *School of Electronic and Electrical Engineering, University of Leeds, Leeds LS2 9JT, UK*

Abstract

Low-energy vibrational modes have been investigated in polycrystalline biphenyl, *para*-terphenyl, *para*-quaterphenyl and *para*-sexiphenyl using THz time-domain spectroscopy (THz-TDS). A number of both internal and external infrared-active modes were observed for wavenumbers ranging between 20 and 80 cm^{-1}. The temperature dependence of these modes is consistent with structural phase transitions occurring in the molecular crystal, indicating that THz-TDS is a sensitive probe of the conformation of conjugated molecular systems.
© 2003 Elsevier B.V. All rights reserved.

1. Introduction

Conjugated polymers [1] and molecules [2] have attracted much interest over the past decade following their effective integration into optoelectronic devices. In these materials, electronic transitions cause a change of molecular conformation and are therefore accompanied by vibrational relaxations. Much effort has been devoted to the study of higher-energy vibrational modes (with wavenumber $\bar{v} \approx 500$–2000 cm^{-1}) such as C–C on-ring and inter-ring stretches which dominate the emission and absorption spectra of conjugated polymers and oligomers [3]. In contrast, comparatively little is known about the low-energy ($\bar{v} < 100$ cm^{-1}) vibrational modes and their influence on the exciton relaxation dynamics and the fluorescence lineshape. Recent calculations have indicated that consideration of low-energy vibrational modes (e.g. torsional twisting and chain stretching) is essential for a correct modelling of the emission spectra of phenylene vinylene [4] and phenylene [5] oligomers. Similarly, the inclusion of low-energy modes was shown to be necessary for an accurate description of the energy relaxation dynamics in films of poly(phenylene vinylene) under site-selective excitation conditions [6]. Furthermore, exciton diffusion in conjugated polymer

---

films has been established to be a temperature-activated process, with an activation energy of the order of a few THz [7] which suggests that low-energy vibrational modes need to be included for a correct description of exciton and charge-carrier diffusion in conjugated polymer films.

Previous vibrational spectroscopy in the low-energy range has largely been conducted by the study of Raman scattering, while access to information about infra-red (IR) active modes has been hampered by the lack of strong far-IR sources and detectors [8]. However, the recently developed technique of THz time-domain spectroscopy (THz-TDS) [9,10] has opened up access to the THz-frequency range of the electromagnetic spectrum, allowing far-IR transmission spectroscopy with wide dynamic range. Unlike incoherent far-IR Fourier-transform spectroscopy (FTIR), THz-TDS relies on the coherent generation and detection of THz-pulses with durations of less than one picosecond. The technique may therefore be extended to probe time-resolved transmission changes following electronic transitions induced by a pump pulse in the visible part of the spectrum [11].

In the study presented here, we have performed THz-TDS on a series of phenylene oligomers in polycrystalline form to investigate their IR-active vibrational modes below 90 cm^{-1} for a range of temperatures. Oligo(*para*-phenylenes) are an important class of conjugated materials, with the shorter oligomers being used as efficient laser dyes [12] and the more extended oligomers (such as *para*-sexiphenyl) being implemented in organic light-emitting diodes [13,14].

2. Materials and experimental technique

Polycrystalline powders of biphenyl (2P), *para*-terphenyl (3P) and *para*-quaterphenyl (4P) were purchased from Sigma–Aldrich, *para*-sexiphenyl (6P) from Tokyo Chemical Industry (TCI). All materials were used without further purification. Measurements taken for *para*-terphenyl were repeated using materials from another source [1] and

---

[1] An alternative supply of *para*-terphenyl was kindly provided by Dr. M. S. Khan, Department of Chemistry, Sultan Qaboos University, P.O. Box 36, Al Khod 123, Sultanate of Oman.

identical results were obtained. Samples were prepared by blending each phenylene oligomer with polyethylene powder in a mass ratio of 1:9 and subsequently forming pellets of ≈2.2 mm thickness under application of a pressure of 40 MPa. Polyethylene is largely transparent in the THz-region of the electromagnetic spectrum [15], however, all measurements were made with reference to a sample consisting solely of polyethylene.

Far-infrared spectra were obtained using THz-TDS [16,17]. A schematic diagram of the experimental setup is shown in Fig. 1. Samples were held in a helium flow cryostat with an accessible temperature range of 1.5–300 K and kept in a low pressure helium environment for all measurements. The far-IR optics of the spectrometer were purged with dry nitrogen gas to reduce atmospheric absorption. Single-cycle far-IR (THz) pulses were generated using a 2 mm thick GaAs photoconductive switch [18,19], which was biased with a 20 kHz, bipolar (±100 V) square wave. The
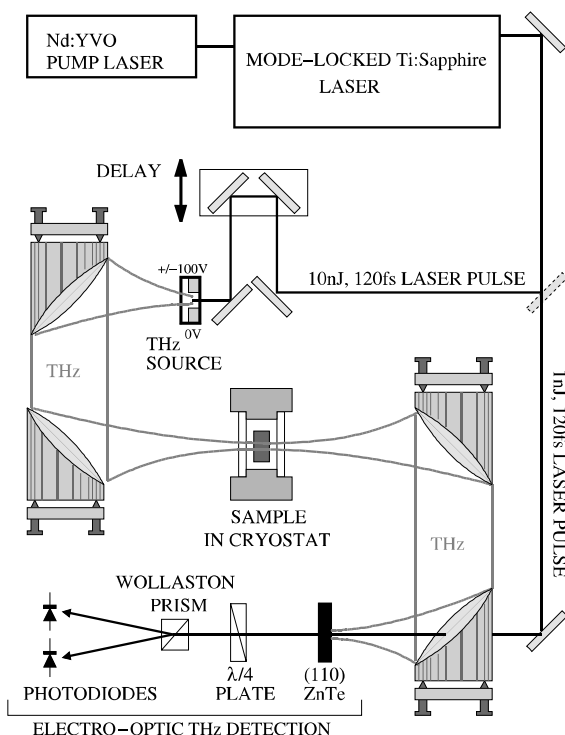

Fig. 1. Schematic diagram of the optical arrangement used for THz-TDS measurements.

1-mm gap between the gold electrodes of the switch was illuminated with 800 nm, 120 fs, 10 nJ pulses from a mode-locked Ti:sapphire laser. The THz pulses, after transmission through the sample, were detected using electro-optic sampling [20]. This detection used a delayed (1 nJ) part of the original Ti:sapphire laser pulse to probe the electric field in a 1-mm thick (1 1 0)-ZnTe crystal as a function of time. Both low and high resolution spectra were measured for each sample. The low resolution (1.67 cm^{-1}) spectra were particularly suitable for identifying modes as the temporal range of the measurement was short enough (20 ps) to avoid spectral artefacts caused by multiple THz reflections in the pellet. High-resolution (0.25 cm^{-1} or 7.5 GHz) scans over a longer delay range were then performed to measure the linewidths of the absorption features identified from the low resolution spectra.

The raw time-domain electric field data, $E_s(t)$, measured from the sample and those of the reference, $E_r(t)$, were zero-filled (as is common in FTIR analysis) and Fourier transformed to give $\tilde{E}_s(\omega)$ and $\tilde{E}_r(\omega)$. These data were then divided to give an amplitude transmission function:

$$\tilde{T}(\omega) = \frac{\tilde{E}_s(\omega)}{\tilde{E}_r(\omega)} = \frac{|\tilde{E}_s(\omega)|e^{i\phi_s(\omega)}}{|\tilde{E}_r(\omega)|e^{i\phi_r(\omega)}}, \quad (1)$$

where $||$ denotes the modulus and $\phi_s(\omega)$ and $\phi_r(\omega)$ are the frequency dependent phases of the sample and reference electric fields, respectively. The absorbance α and refractive index n were then calculated according to

$$\alpha(\omega) = -\frac{2}{rd} \ln \left| \frac{\tilde{E}_s(\omega)}{\tilde{E}_r(\omega)} \right|, \quad (2)$$

$$\Delta n(\omega) = \frac{cd}{\omega} [\phi_s(\omega) - \phi_r(\omega)], \quad (3)$$

where r is the volume fraction of sample in the pellet, d is the thickness of the pellet and c is the speed of light. $\Delta n(\omega)$ is the difference between the polyethylene pellet with and without the polycrystalline sample included. In this analysis, we assume that the the Fresnel coefficients of the sample and reference pellet are the same, which is justified as $\Delta n < 0.04$ in all our measurements.

3. Results and discussion

The relative orientation of adjacent phenyl rings is of great significance for the electrical and optical properties of oligo(*para*-phenylenes) and conjugated polymers, many of which contain an interring C–C bond as part of their structural repeat unit. If the phenyl rings are predominantly in the same plane, an increased overlap of their π-orbitals will result in a more strongly delocalised exciton or an increased intrinsic conjugation length. In gas, melt and solution phases, oligo(*para*-phenylene) have large dihedral angles (30–40°) between neighbouring phenyl-ring planes owing to the repulsion between hydrogen atoms in the *ortho* positions [21]. In contrast, the solid polycrystalline and spin-cast polymer forms tend to be more planar at room temperature as a result of intermolecular interactions. However, neutron scattering [22], X-ray diffraction [22], ultraviolet-absorption spectroscopy [23] and Raman studies [24,25] of crystalline oligo(*para*-phenylenes) have indicated that this degree of planarisation is temperature dependent. Phase transitions have been observed in polycrystalline 2P, 3P and 4P at critical temperatures of 40, 193 and 238 K, respectively [22].

THz-absorption measurements of organic crystals provide information on both molecular conformation and the intermolecular environment. The two main conformations of oligo(*para*-phenylenes) are the planar form, with point group symmetry *mmm* (D$_{2h}$), and the non-planar 222 (D$_2$) form where the phenyl rings are twisted with respect to each other. By considering molecular symmetry, these forms can clearly be distinguished since the vibrational modes of the two conformations are described by different irreducible representations and hence selection rules. However, in the solid state, it is also necessary to consider the symmetry of the crystal, where the intramolecular (internal) vibration of the molecule is constrained by the crystal symmetry, requiring factor group analysis. Furthermore, low-energy lattice vibrations and librations cause the appearance of intermolecular (external) modes. Planar organic molecules, such as the oligo(*para*-phenylenes), tend to form monoclinic crystals belonging to the

$P2_1/a$ space group [22]. Hence, the factor groups for the planar and non-planar molecules in the crystal are $2/m$ (C_{2h}) and 2 (C_2), respectively. It should be noted that for the C_{2h} factor group the vibrational modes described by the *ungerade* irreducible representations ($A_u + B_u$) are IR active, while the *gerade* ($A_g + B_g$) representations are inactive. In contrast, the irreducible representations ($A + B$) of the C_2 factor group are all IR active. Thus IR activity can be used to study phase transitions between planar (C_{2h}) and non-planar (C_2) oligo(*para*-phenylene) organic crystals.

Figs. 2 and 3 show the IR absorption spectra of polycrystalline 2P, 3P, 4P and 6P samples measured at 10 K using THz-TDS. The presence of the absorption features is confirmed by the observa-
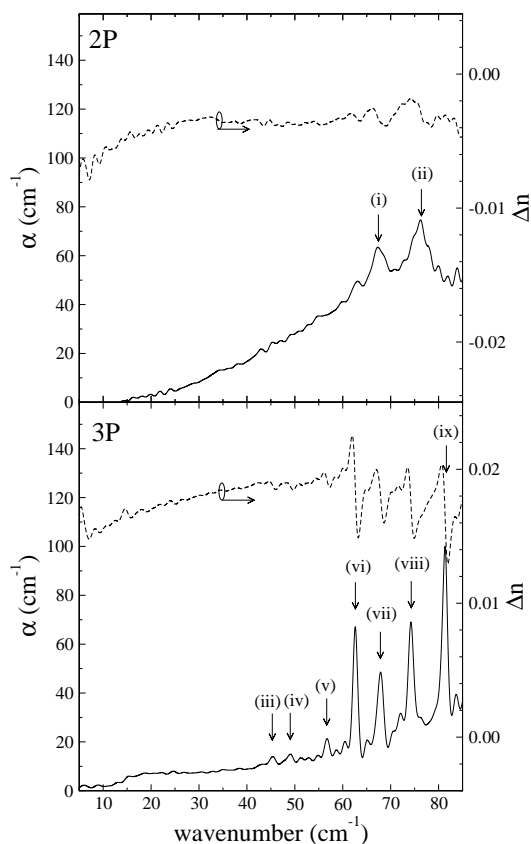

Fig. 2. THz absorption α (solid line) and refractive index change Δn (dashed line) at 10 K as a function of photon wavenumber for biphenyl (2P) and *para*-terphenyl (3P).
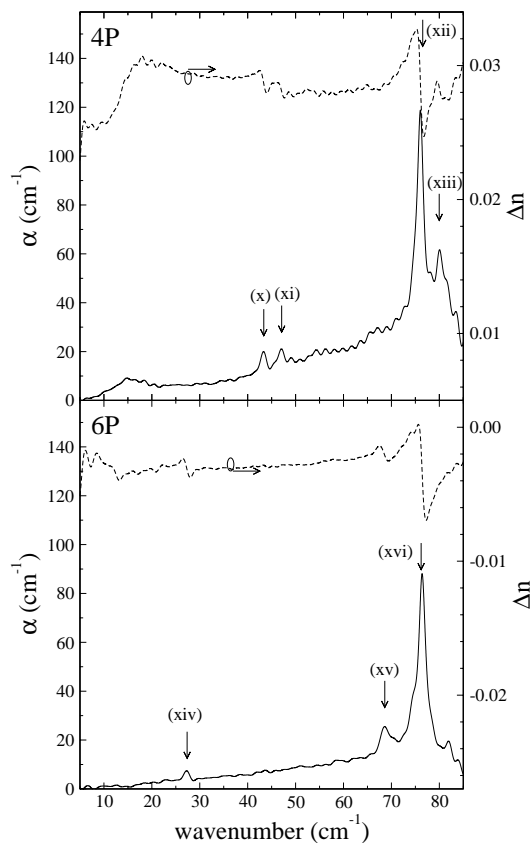

Fig. 3. THz absorption α (solid line) and refractive index change Δn (dashed line) at 10 K as a function of photon wavenumber for *para*-quaterphenyl (4P) and *para*-sexiphenyl (6P).

tion of changes in the refractive index (indicated by the dashed lines), in agreement with Kramers–Kronig relations. We have identified vibrational modes with wavenumbers in the range between 27 and 82 cm^{-1} which are labelled from (i) to (xvi) in Figs. 2 and 3. A summary of our results is given in Table 1 where the modes marked in the figures are listed together with the linewidths of major modes obtained from high resolution spectra (not shown). For the shorter oligomers we have assigned most of the observed modes through comparison with previous experimental results based on Raman or IR spectroscopy or neutron scattering measurements (see references given in the table). We have then extrapolated these results to the longer oligomers thereby providing a tentative

Table 1
List of low-energy vibrational modes for polycrystalline biphenyl, *para*-terphenyl, *para*-quaterphenyl and *para*-sexiphenyl at a temperature of 10 K

Mode	$\bar{v}$ (cm^{-1})	$\Delta\bar{v}$ (cm^{-1})	Representation	Tentative assignment	Reference
2P (biphenyl)					
(i)	67.4	3.1	A_u	Internal long-axis torsion	[5,28,29]
(ii)	76.2	4.2	$A_g + B_g$	External libration	
3P (*p*-terphenyl)					
(iii)	45.4		$A_g + B_g$	External libration	[27]
(iv)	49		$A_g + B_g$	External libration	[27]
(v)	56.7			External translation	[27]
(vi)	62.6	0.77	B_u	Internal in-plane scissoring	
(vii)	68.0	1.2	A_g	Internal in-plane scissoring	[27]
(viii)	74.3	1.2	A_u	Internal long-axis torsion	[5,27]
(ix)	81.3	0.94	A_u	Internal out-of-plane scissoring	[27]
4P (*p*-quaterphenyl)					
(x)	43.4		$A_g + B_g$	External libration	
(xi)	47.0		$A_g + B_g$	External libration	
(xii)	76.0	1.7	A_u	Internal long-axis torsion	[5]
(xiii)	80.2				
6P (*p*-sexiphenyl)					
(xiv)	27.2		$A_g + B_g$	External libration	
(xv)	68.6				
(xvi)	76.5	1.5	A_u	Internal long-axis torsion	[5]

Tentative assignments of modes were obtained from geometric considerations and by comparison with previous computational and experimental studies. $\Delta\bar{v}$ represents the full-width-at-half-maximum of an absorption peak when the background absorption is subtracted, and was obtained from the high resolution spectra (not shown).

assignment to some of their modes. However, some of the modes remain unidentified, and detailed quantum chemical calculations are required in order to provide further information about the origin of these modes. Such calculations will have to include the effects of the crystal potential in order to account for the existence of external modes and to give an accurate description of the frequencies of internal modes. The irreducible representations for the assigned modes given in the table are for a factor group corresponding to the molecules in a planar conformation (C_{2h}).

We have identified ring-torsional modes at 67.4, 74.3, 76.0, and 76.5 cm^{-1} for 2P, 3P, 4P and 6P, respectively. These modes are particularly important since $\pi \rightarrow \pi^*$ transitions in these materials induce a planarization of the molecule and therefore interact strongly with ring-torsions. Consequently these modes must be considered for a correct description of the electronic ($S_0 \leftrightarrow S_1$) absorption and emission spectra. Such a treatment

has recently been presented by Karabunarliev et al. [5] who have used quantum chemical calculations to determine vibrational frequencies for C–C-stretch, ring-stretch, and inter-ring torsional modes in a series of phenylene oligomers. The authors of this study calculated ring-torsional modes at 61, 75, 80 and 84 cm^{-1} for 2P, 3P, 4P and 6P, respectively. Comparison with our experimental results show that this quantum chemical treatment results in an underestimate of the ring-torsional frequencies for biphenyl (2P) and an overestimate for oligomers longer than *para*-terphenyl (3P). Karabunarliev et al. [5] observed a similar trend in the discrepancy between the calculated and experimental values for the optical ($S_0 \leftrightarrow S_1$) transition energies. Differences between our measurements and the quantum chemical study are to be expected as the calculations were performed considering isolated molecules while our measurements were taken for polycrystalline materials. Transitions between the solid, liquid or

gas phases of biphenyl have been experimentally shown to induce shifts of the order of a few cm^{-1} for low-energy vibrational modes [26]. For a more accurate theoretical description of the vibrational frequencies of low-energy modes the crystal potential will therefore have to be taken into account. Furthermore, the semi-empirical nature of the Hamiltonian and the incomplete treatment of configuration interactions in the calculations described in [5] will also result in deviations from the experimental results. Our comprehensive measurement of these low-energy vibrational modes for a range of phenylene oligomer should therefore provide an idea starting point for further refinement of quantum chemical models.

Fig. 4 shows the temperature dependence of the THz absorption spectra from 2P, 3P and 4P samples. For 2P, the absorption features (i) and (ii)
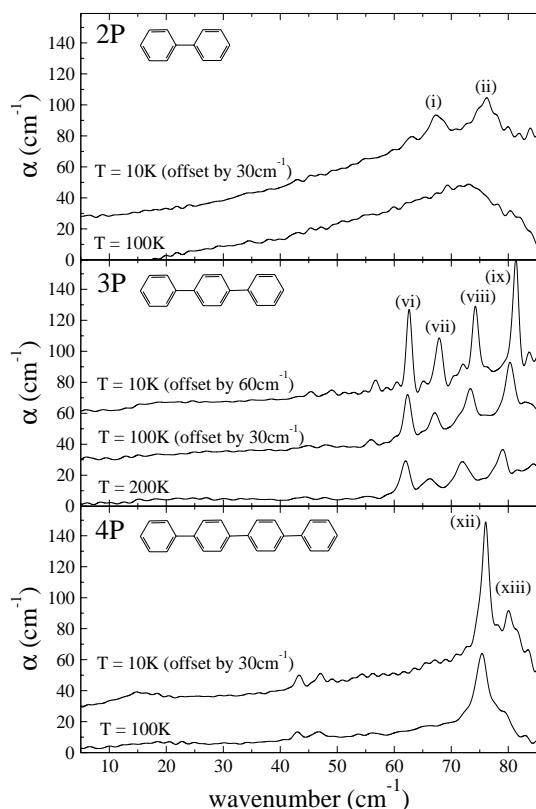

Fig. 4. Temperature dependence of the THz absorption spectra of biphenyl (2P), *para*-terphenyl (3P) and *para*-quaterphenyl (4P). (Spectra have been offset for clarity.)

become indistinct above the critical temperature of 40 K, which is probably a result of a reduction in the oscillator strength of the (IR-active) A_u torsional mode as the molecules in the crystal becomes more planar. However, for the 3P crystal, the absorption features (vi)–(ix) are still clearly observable above the 193-K critical temperature. In particular, mode (vii) is still present although it has been assigned an IR-inactive A_g representation. It has been suggested that the phase transition for 3P is an order–disorder type [22], where the molecules remain non-planar (D_2) even above the transition temperature. Thus the high temperature phase is only planar *on average*, consisting of approximately equal proportions of twisted conformations with no change to the selection rules. Our results are therefore consistent with the existence of different types of phase transitions in the two materials. In addition it should be noted that the absorption features of oligo(*para*-phenylene) in general tend to shift to lower frequencies as the temperature is increased. This reflects the response of the lattice, which also couples to many of the internal modes. It is interesting to note that mode (vi) in 3P is relatively insensitive to temperature. This indicates that it corresponds to an internal mode which is not influenced significantly by, and is therefore weakly coupled to, the lattice. This observation is in contradiction with an earlier assignment of this mode to external translations [27]. Similarly, the frequencies of the ring-torsional modes in 3P (viii) and 4P (xii) are found not to shift strongly below their respective phase-transition temperatures.

4. Conclusions

We have performed an investigation into the low-energy vibrational modes of oligo(*para*-phenylenes) in polycrystalline form. The high sensitivity of THz time-domain spectroscopy has allowed us to determine a range of IR active modes which we have assigned to specific internal and external vibrations. In particular, we have measured the energies of ring-torsional modes which couple strongly to the optical ($S_0 \leftrightarrow S_1$) transitions in these materials. We have further shown that the

temperature dependence of these modes is a sensitive probe of the phase transitions occurring in these systems. THz-TDS is thus a valuable technique for investigating molecular conformation in conjugated polymer systems. Furthermore, this technique may be extended to a visible-pump/THz-probe measurement in which changes in the vibrational modes with optical excitation can be deduced. Subsequent analysis of such studies, correlated with quantum chemical calculations should provide experimental insight into the excited-state geometry in these molecular systems.

Acknowledgements

References

[1] R.H. Friend, R.W. Gymer, A.B. Holmes, J.H. Burroughes, R.N. Marks, C. Taliani, D.D.C. Bradley, D.A. Dos Santos, J.L. Bredas, M. Logdlund, W.R. Salaneck, Nature 397 (6715) (1999) 121.

[2] M.D. Watson, A. Fechtenkötter, K. Müllen, Chem. Rev. 101 (5) (2001) 1267.

[3] B. Tian, G. Zerbi, K. Müllen, J. Chem. Phys. 95 (5) (1991) 3198.

[4] S. Tretiak, A. Saxena, R.L. Martin, A.R. Bishop, Phys. Rev. Lett. 89 (9) (2002) 097402.

[5] S. Karabunarliev, E.R. Bittner, M. Baumgarten, J. Chem. Phys. 114 (13) (2001) 5863.

[6] S.P. Kennedy, N. Garro, R.T. Phillips, Phys. Rev. B 64 (11) (2001) 115206.

[7] E.J.W. List, C. Creely, G. Leising, N. Schulte, A.D. Schlüter, U. Scherf, Müllen, W. Graupner, Chem. Phys. Lett. 325 (2000) 132.

[8] R.E. Miles, P. Harrison, D. Lippens (Eds.), Terahertz sources and systems, Kluwar Academic Publishers, Dordrecht, 2001.

[9] D. Grischkowsky, S. Keiding, M. Vanexter, C. Fattinger, J. Opt. Soc. Am. B 7 (1990) 2006.

[10] B. Ferguson, X.C. Zhang, Nature Mater. 1 (1) (2002) 26.

[11] R. Huber, F. Tauser, A. Brodschelm, M. Bichler, G. Abstreiter, A. Leitenstorfer, Nature 414 (2001) 286.

[12] H.W. Furumoto, H.L. Ceccon, IEEE J. Quantum Electron. 6 (1970) 262.

[13] N. Koch, A. Pogantsch, E.J.W. List, G. Leising, R.I.R. Blyth, M.G. Ramsey, F.P. Netzer, Appl. Phys. Lett. 74 (20) (1999) 2909.

[14] C. Hosokawa, H. Higashi, T. Kusumoto, Appl. Phys. Lett. 62 (25) (1993) 3238.

[15] E.D. Palik (Ed.), Handbook of Optical Constants of Solids, Academic Press, New York, 1985.

[16] M. Walther, B. Fischer, M. Schall, H. Helm, P. Uhd Jepsen, Chem. Phys. Lett. 332 (2000) 389.

[17] Y.C. Shen, P.C. Upadhya, E.H. Linfield, A.G. Davies, Appl. Phys. Lett. 82 (14) (2003) 2350.

[18] G. Zhao, R.N. Schouten, N. van der Valk, W.T. Wenckebach, P.C.M. Planken, Rev. Mod. Instrum. 73 (4) (2002) 1715.

[19] Y.C. Shen, P.C. Upadhya, A.G. Davies, E.H. Linfield, in: J.M. Chamberlain, A.G. Davies, P. Harrison, E.H. Linfield, R.E. Miles, S. Withington (Eds.), Proceeding of 2002 IEEE Tenth International Conference on Terahertz Electronics, IEEE, Piscataway, USA, 2002, pp. 165–168.

[20] D.H. Auston, M.C. Nuss, IEEE J. Quantum Electron. 24 (2) (1988) 184.

[21] S. Guha, W. Graupner, R. Resel, M. Chandrasekhar, H.R. Chandrasekhar, R. Glaser, G. Leising, Phys. Rev. Lett. 82 (18) (1999) 3625.

[22] J.L. Baudour, Acta Cryst. B 47 (1991) 935.

[23] T. Suzuki, G. Kudo, K. Nukui, M. Mizuno, K. Abe, T. Shigenari, J. Lumin. 87–89 (2000) 623.

[24] S. Guha, W. Graupner, R. Resel, M. Chandrasekhar, H.R. Chandrasekhar, R. Glaser, G. Leising, J. Phys. Chem. A 105 (25) (2001) 6203.

[25] P.S. Friedman, R. Kopelman, P.N. Prasad, Chem. Phys. Lett. 24 (1) (1974) 15.

[26] R.M. Barrett, D. Steele, J. Mol. Struct. 11 (1971) 105.

[27] P.A. Reynolds, J.W. White, J. Chem. Soc., Faraday Trans. 68 (1972) 1434.

[28] G. Zerbi, S. Sandroni, Spectrochim. Acta 24A (1968) 483.

[29] K. Krebs, S. Sandroni, G. Zerbi, J. Chem. Phys. 40 (1964) 3503.